Speckle reduction by combination of digital filter and optical suppression in a modified Gerchberg–Saxton algorithm computer-generated hologram

Chien-Yue Chen,[1,*] Qing-Long Deng,[2] Pei-Jung Wu,[3] Bor-Shyh Lin,[3] Hsuan T. Chang,[4] Hone-Ene Hwang,[5] and Guan-Syun Huang[1]

[1]Department of Electronic Engineering, National Yunlin University of Science and Technology, Yunlin 64002, Taiwan

[2]Institute of Photonic Systems, National Chiao Tung University, Tainan 71150, Taiwan

[3]Institute of Imaging and Biomedical Photonics, National Chiao Tung University, Tainan 71150, Taiwan

[4]Department of Electrical Engineering, National Yunlin University of Science and Technology, Yunlin 64002, Taiwan

[5]Department of Electronic Engineering, Chung Chou University of Science and Technology, Yuan-lin 51003, Taiwan

*Corresponding author: chencyue@yuntech.edu.tw

Received 14 March 2014; revised 11 July 2014; accepted 12 July 2014;
posted 14 July 2014 (Doc. ID 207959); published 15 August 2014

A speckleless illuminated modified-Gerchberg–Saxton-algorithm-type computer-generated hologram, which adopts a lower frequency of the iterative algorithm and calculation time, is proposed to code a hologram with two signals and position a multiplexing phase-only function, which can reconstruct the left and the right viewing holograms on the pupillary-distance position after the decryption and still maintain the content with high contrast and definition. The reconstructed image quality presents root mean square error of 0.03, with a diffraction efficiency of 87%, and signal-to-noise ratio of 8 dB after the analysis. Furthermore, two denoising techniques for the digital filter and optical suppression are combined, in which the speckle suppression with pseudorandom phase modulation and a rotating diffuser are utilized for successfully reducing the speckle contrast, which was reduced to below 4%. The goal was to reduce visual fatigue for the viewers.

OCIS codes: (090.1760) Computer holography; (030.6140) Speckle; (110.6150) Speckle imaging; (230.1980) Diffusers.

http://dx.doi.org/10.1364/AO.53.00G163

1. Introduction

Computer-generated holograms (CGHs) based on holography [1] calculate the holographic interference phase patterns with digital signals, utilize a spatial light modulator (SLM) [2] or acousto-optic modulator [3] as the phase pattern recording media, and reconstruct the original three-dimensional (3D) model hologram [4] with the illumination of coherent light. Such a recording process replaces traditional holography with computer generation [5–7]. The advantages are in the reduction of traditional holographic errors and modulation with holographic photosensitive materials [8,9].

Nonetheless, CGH currently encounters three critical issues. First is the problem with speckle. Speckle [10–12] is the interference that results from high coherence of the laser and the topography of an object's surface. When coherent light illuminates a rough surface, the original coherent length is destroyed so that the scattered light is reflected by the object, received by the detector, and appears as constructive interference and destructive

1559-128X/14/27G163-06$15.00/0

interference. This further affects the speckle patterns, resulting in random brightness–darkness distribution, which not only reduces the contrast and definition of the projected image, but also causes serious dizziness and visual fatigue for viewers [13]. Second is the image size and angle of view. The common pixel size of SLMs (~8 μm) limits the CGH size and the angle of view. Last is the issue of CGH computing speed. In order to calculate the phase distribution of each 3D spatial coordinate in hologram, the large amount of data requires longer computing time.

To solve the above problems, a modified Gerchberg–Saxton algorithm (MGSA) is proposed for CGH phase coding. A Fresnel diffraction core algorithm is applied in MGSA, which enhances the image quality of a hologram [14]. In addition, the MGSA can simultaneously compute the position multiplexing distribution [15] to distribute the decoded images at distinct positions for viewing from multiple angles of view. In comparison with traditional CGH, a single multiplexing phase algorithm largely reduces the number of phase iterative times as well as the length of time of a hologram. As the decoded images can be distributed to distinct positions with multiplexing, the images of the left and the right angles of view are input to the head-mounted display (HMD) and, through virtual image projection, they allow the viewer to view a large-size CGH.

Regarding the reduction of speckle, two denoising techniques for digital filtering and optical suppression are combined. First of all, the pseudorandom phase mask [16] function is included in the MGSA and phase filters are sequentially provided in the iterative process. A rotation diffuser is placed on the intermediate image plane [17,18] in the optical reconstruction projection as a secondary means of reducing interference to reduce the speckle intensity distribution. From the experimental results, the speckle contrast (SC) is reduced to 3.9%, so that it can be ignored by human eyes [19].

2. Generation of a Hologram Pattern

A. Principle of the MGSA

The MGSA is utilized in this study for rapidly calculating the complete phase wave function, where Fresnel transform (FrT) is used for repeatedly iterating the phase between objects to modify the phase difference [20,21]. Different from traditional Gerchberg–Saxton algorithm [22], this can enhance the computing speed. In addition, it is proposed that a random phase is included in the beginning of the algorithm to reduce the mutual interference of the phase that results from the synthesis among multiple images and decreases the decoding error caused in the image reconstruction. Furthermore, phase modulation is first applied to calculating the position multiplexing distribution, in which fewer iteration times are maintained and the error between the approximate function and the target function is reduced.

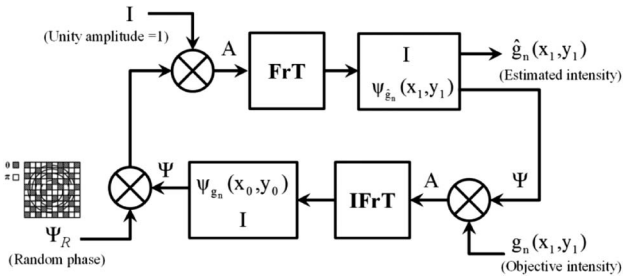

Fig. 1. Block diagram of a MGSA.

Figure 1 shows the block diagram of the MGSA. A random phase function is first generated by inputting $\psi_{gn}(x_0,y_0)$. In the system, n is the holograms of the left and the right angles of view. The phase function $\psi_{\hat{g}n}(x_0,y_0)$ is then multiplied by the initial amplitude for the Fresnel transform (FrT) so as to acquire the approximate image phase function $\hat{g}_n(x_1,y_1)$ and the approximate phase function $\psi_{\hat{g}n}(x_1,y_1)$. Third, the phase function $\psi_{gn}(x_0,y_0)$ is acquired with an inverse Fresnel transform (IFrT) of the target image function $g_n(x_1,y_1)$ and the approximate phase function $\psi_{\hat{g}n}(x_1,y_1)$. Meanwhile, a pseudorandom phase mask function Ψ_R proceeds the phase deviation. For the accuracy of the approximate image, the second and the third steps are repeated for the image iteration, and this continues until the approximate image function $\hat{g}_n(x_1,y_1)$ and the target image function $g_n(x_1,y_1)$ are relatively consistent. The approximate image phase function $\psi_{\hat{g}n}(x_1,y_1)$ is then outputted, and the coded image is the phase-only function (POF).

Equation (1) is the Fresnel integration formula, where $E(x,y,z)$ is the coordinate of the original image field, $E(x',y',0)$ the coordinate of the diffracted hologram of the original image through FrT, λ the wavelength of incident light, z the distance between the hologram and the image in the defined space, p the spatial frequency at the x direction, and q the spatial frequency at the y direction:

$$E(x,y,z) = \frac{\exp(j2\pi z/\lambda)}{j\lambda z}\exp\left[\frac{j\pi}{\lambda z}(x^2+y^2)\right] \times \mathrm{FrT}\left\{E(x',y',0)\exp\left[\frac{j\pi}{\lambda z}(x'^2+y'^2)\right]\right\}, \tag{1}$$

where $p = (x/\lambda z)$; $q = (y/\lambda z)$.

B. Spatial Phase Modulation and Synthesis

Each pixel in the CGH could be regarded as the phase information of the target image which is formed by the interference of object light and reference light. The modulation of pixel distribution is equivalent to changing light interference. In other words, a modulated pixel block would change the image spatial position during reconstruction, as shown in Fig. 2. The holograms of the left and the right angles of view correspond to the binocular distance of human

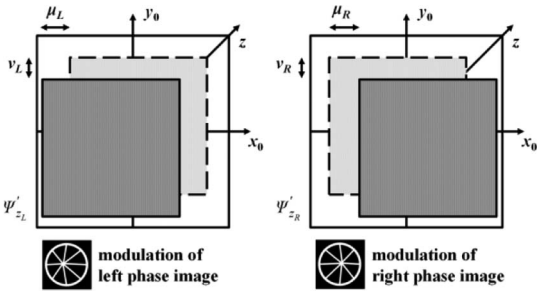

Fig. 2. Spatial phase modulation.

vision. The light gray block is the originally coded POF. After spatial phase modulation, the diffraction light spatial distribution is changed so that the target image transforms to a distinct spatial position (dark gray block) to complete the position multiplexing distribution. The phase modulation equations are shown as Eqs. (2) and (3). The approximate image function $\hat{g}_{zn}(x_1,y_1)\exp[\varphi_n(x_1,y_1)]$ is proceeded by the phase modulation based on the deviation formula $(\mu_n,\upsilon_n) = (\alpha_n D_w,\beta_n D_h)$, where μ_n is the offset factor at the x direction, υ_n the offset factor at the y direction, and D_w and D_h the width and height factors of the approximate image, respectively. The phase modulation signal $\psi'_{Zn}(x_0,y_0)$ is acquired after the transformation. Finally, several phase signals are recorded in the same hologram, according to the phase synthesis equation Eq. (4). $A_s^z(x_0,y_0)\exp[j\psi_s^z(x_0,y_0)]$ is the total amplitude intensity and phase information of the hologram.

$$\mathrm{FrT}\{\exp[j\psi'_{Z_n}(x_0,y_0)];\lambda;z_S\} = \hat{g}_n^z(x_1\pm\mu_n,y_1\pm\upsilon_n)\exp[j\varphi_n(x_1,y_1)], \quad (2)$$

$$\psi'_{Z_n}(x_0,y_0) = j\psi_{z_n}(x_0,y_0) + \frac{2\pi(\mu_n x_0+\upsilon_n y_0)}{\lambda z_s}, \quad (3)$$

$$A_s^z(x_0,y_0)\exp[j\psi_s^z(x_0,y_0)] = \exp[j\psi'_{Z_n}(x_0,y_0)] + \exp[j\psi'_{Z_{n+1}}(x_0,y_0)]. \quad (4)$$

3. Experiments and Analysis

Figure 3 shows the MGSA-type CGH coding and the multiview reconstruction. In the MGSA-type CGH coding process, the image size is 1000 pixel × 1000 pixel, the wavelength band is 532 nm, and the diffractive hologram distance is 600 mm. To conform to the binocular viewing position, the left and the right viewing holograms are set at 1.5 offset on the x axis, while no offset is present on the y axis. The POF of the left and right viewing holograms is further edited with Eqs. (1)–(4).

The prototype of a speckleless illuminated MGSA-type CGH system with a VIS DPSS laser (532 nm, 26 mW) is shown in Fig. 4. The SLM (WUXGA, 8.1 μm, HOLOEYE) records the POF, which is encoded with the POF of the combined left and right

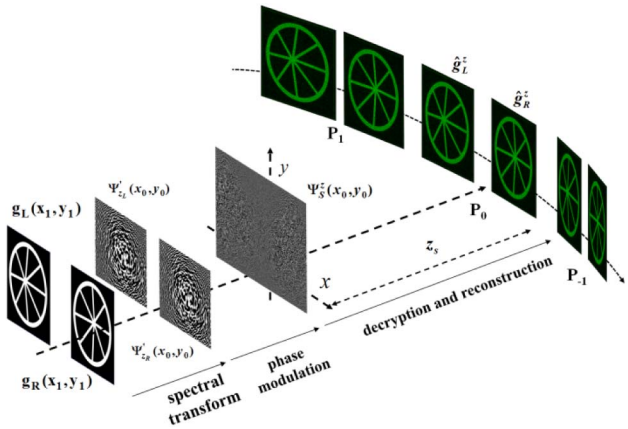

Fig. 3. Schematic diagram of the MGSA-type CGH coding and multiview reconstruction.

viewing holograms by the MGSA, and then reconstructs the images by using coherent light. Lens_2, Lens_3, and Lens_4 are the projection modules that generate a real image with 6.11 magnifications. A diffuser [size 50 mm × 50 mm, surface roughness average (R_a) 1.57 μm], which is made by grinding Al_2O_3 powder, is placed on the intermediate image plane to reduce speckles. Finally, the left viewing hologram and the right viewing hologram are projected to CCD cameras and transmitted to the HMD to view the largest visual holograms. With the characteristics of rotating diffusers, the speckle that is caused from the partly noncoherent light would be reduced. Figure 5 shows a pair of CGHs after decryption. With cyclopean vision [23], the stereo image in the figure would extrude the screen when the dot viewed by both eyes would be convergent to a point.

A. Analysis of Reconstruction Image

To effectively acquire the image quality of a MGSA-type CGH after decryption, a computer computation is first utilized for evaluating the decrypted image with the following methods from Eqs. (7)–(9). First, the root mean square error (RMSE) [24] is defined as the average difference between the original image and the reconstructed image of each pixel. Second, the signal-to-noise ratio (SNR) [25] is defined as the power ratio between the signal (I_S) and the

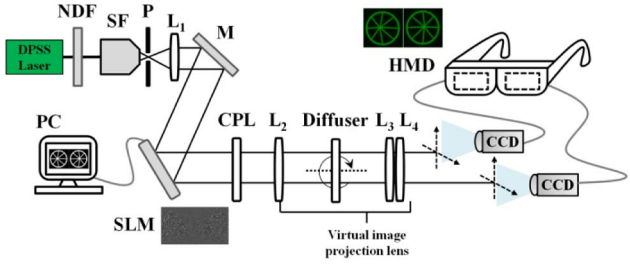

Fig. 4. Diagram of prototype speckleless illuminated MGSA-type CGH system. NDF, neutral density filter; SF, spatial filter; P, pinhole; L_1–L_4, lenses; M, mirror; CPL, circular polarizer lens; SLM, spatial light modulator; HMD, head-mounted display.

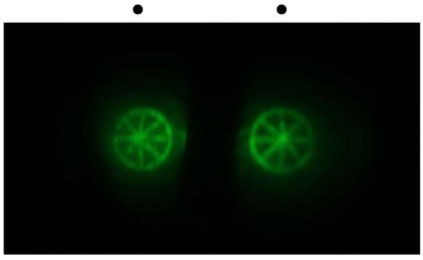

Fig. 5. Speckleless illuminated MGSA-type CGH pair.

background noise (I_N). Third, the relative diffraction efficiency (DE) [26] is defined as the intensity proportion of the diffracted image signal to all the signals in the reconstructed image, where ΣI_S is the total intensity of the reconstructed image signals, and ΣI_N the total intensity of the reconstructed image noise.

$$\mathrm{RMSE} = \left[\left(\sum I_N^2\right)/MN\right]^{1/2}, \tag{7}$$

$$\mathrm{SNR} = 10 \times \log_{10}(I_S/I_N), \tag{8}$$

$$DE = \sum_S I_S \Big/ \left(\sum_S I_S + \sum_N I_N\right) \times 100\%, \tag{9}$$

where MN is the resolution of image size, I_S is the signal power, and I_N is the noise power

Figure 6 shows the quality analysis of the reconstructed image simulated by a MGSA-type CGH and the reconstructed image in the experiment. The POF is acquired 10 times with the MGSA iterative method, with the average calculation time being 60.28 s, and the contents are compared with other iterative Fourier or Fresnel transform algorithm (IFTA) [26]. Figure 6(a) shows RMSE, in which the reconstructed image simulated by the MGSA-type CGH and the reconstructed image in the experiment show that the analysis value is lower than 0.03, presenting a reconstructed image that conforms to the simulation algorithm. Figure 6(b) shows DE; the reconstructed image efficiency (86.80%) is slightly lower than that of the reconstructed image by simulation (95.21%), but the intensity is in the acceptable range of human eyes. Figure 6(c) shows the SNR, which is about 9.97 dB in the reconstructed image by simulation, but 8.06 dB in the reconstructed image in the experiment, revealing the quality has been reduced with the diffraction of the diffuser.

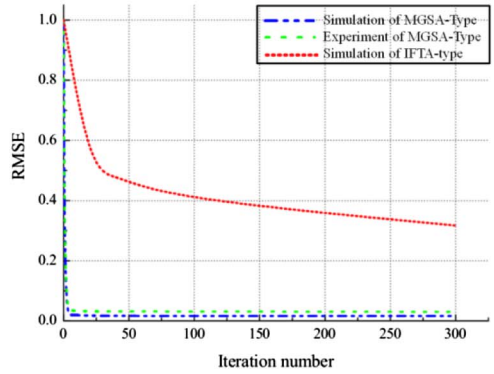

(a)

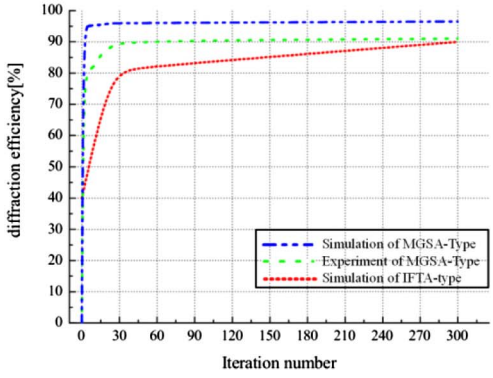

(b)

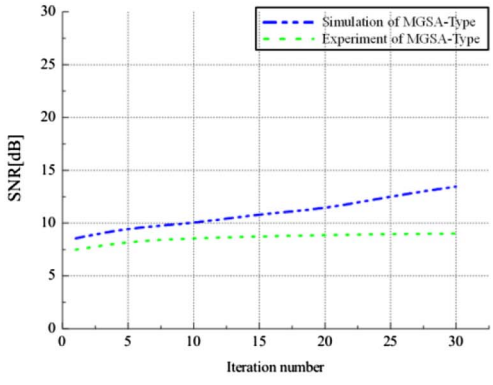

(c)

Fig. 6. Evaluation of the reconstructed image by simulation and the reconstructed image in the experiment: (a) RMSE, (b) DE, and (c) SNR.

B. Analysis of Speckle

The inclusion of the MGSA in the function of a pseudorandom phase mask is proposed in this study, in which phase masks are sequentially used in the iterative process to precede the preliminary noise reduction with such a digital filter. In the optical reconstruction projection, a rotating diffuser is placed in the intermediate plane to do the second speckle denoising which is the optical suppression. Actually, when the laser passed through the diffuser, the randomly distributed surface disturbed the wavefront of the laser and high coherency to form uniform scattering light. As for the phase, the initial phase would become a random phase distribution after passing through the diffuser. Moreover, at the rotating diffusers, the laser would appear as uniformly but partly noncoherent light so that the speckle would be reduced. Consequently, SC is defined as the speckle levels by using Eq. (10), when the range appears in 0–1 [27,28]:

$$\text{speckle contrast} = \frac{\sqrt{\langle I^2\rangle - \langle I\rangle^2}}{\langle I\rangle} \times 100\%. \tag{10}$$

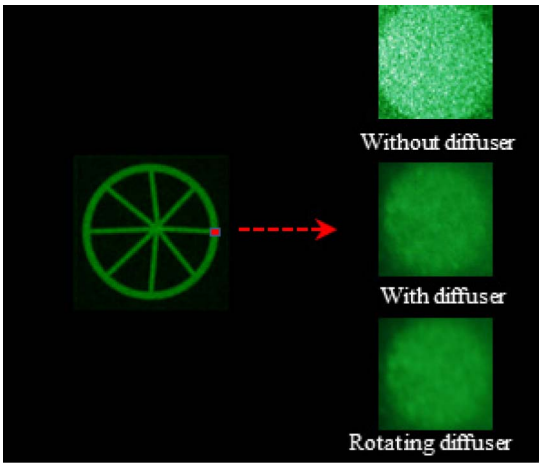

Fig. 7. Speckle distributions with pseudorandom phase modulation (top inset), with pseudorandom phase modulation and a diffuser (middle inset), and with pseudorandom phase modulation and a diffuser rotating at a speed of 2π rad/s (bottom inset).

Here, I is the light intensity, which is the square of the absolute value of the light signal. Figure 7 shows the speckle pattern shot by a CCD camera with ISO 200, focal length 55 mm, and aperture f/2.8.

To conform to the observation of human eyes, the integral time of the CCD camera must be equivalent to that of human eyes (1/60–1/30 s) [29]. Referring to a previous study [18], the SC of the original image is larger than 50%; however, in this study, the reconstructed images with pseudorandom phase give a SC of 19.01% (see Fig. 7). With a static diffuser, the speckle distribution is reduced by about 1/3 and the SC is 7.12% (see Fig. 7). When the diffuser is rotated with a speed of 2π rad/s, the SC is reduced to 3.90% (see Fig. 7), which can be ignored by human eyes because the SC is under 4% [10]. Light intensity distribution is further evaluated, as shown in Fig. 8, in which the rotating diffuser is used for equalizing the random speckle distribution and effectively reducing the SC.

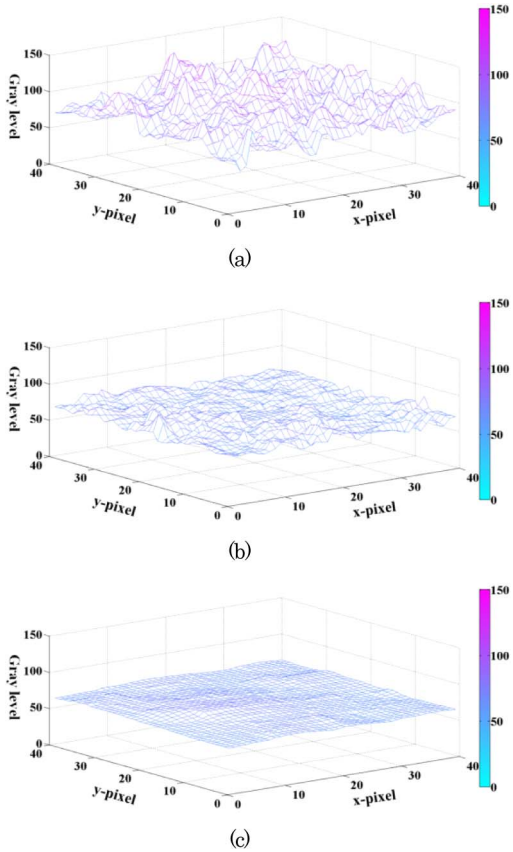

Fig. 8. Light intensity distributions (a) with pseudorandom phase modulation, (b) with pseudorandom phase modulation and a diffuser, and (c) with pseudorandom phase modulation and a diffuser rotating at a speed of 2π rad/s.

4. Conclusion

A speckleless illuminated MGSA-type CGH with higher computing speed that codes left and right viewing hologram phases that function only with an MGSA is proposed in this study. After decryption, the image is projected to positions conforming to pupillary distance. After image quality analysis, the RMSE of the reconstructed image drops below 0.03, and has a DE of about 87% and a SNR of about 8 dB. Moreover, the denoising techniques of the digital filter and optical suppression are also combined to reduce speckle. Pseudorandom phase modulation is also included with a rotating diffuser for light-field destruction, so the speckle contrast can be reduced to below 4% to successfully achieve a speckleless illuminated CGH.

This work is supported by the National Science Council of Taiwan under contract no. NSC 101-2628-E-224-002-MY3.

References

1. D. Gabor, "A new microscopic principle," Nature **161**, 777–778 (1948).
2. N. Hashimoto, S. Morokawa, and K. Kitamura, "Real-time holography using the high-resolution LCTV-SLM," Proc. SPIE **1461**, 291–302 (1991).
3. M. Lucente and T. A. Galyean, "Rendering interactive holographic images," Proc. ACM SIGGRAPH **95**, 387–394 (1995).
4. B. R. Brown and A. W. Lohmann, "Computer-generated binary holograms," IBM J. Res. Dev. **13**, 160–168 (1969).
5. Y. Takaki and N. Okada, "Hologram generation by horizontal scanning of a high-speed spatial light modulator," Appl. Opt. **48**, 3255–3260 (2009).
6. M. Bayraktar and M. Özcan, "Method to calculate the far field of three-dimensional objects for computer-generated holography," Appl. Opt. **49**, 4647–4654 (2010).
7. K. Yamamoto, Y. Ichihashi, T. Senoh, R. Oi, and T. Kurita, "Calculating the Fresnel diffraction of light from a shifted and tilted plane," Opt. Express **20**, 12949–12958 (2012).
8. W. C. Su, C. Y. Chen, and Y. F. Wang, "Stereogram implemented with a holographic image splitter," Opt. Express **19**, 9942–9949 (2011).
9. Q. L. Deng, W. C. Su, C. Y. Chen, B. S. Lin, and H. W. Ho, "Full color image splitter based on holographic optical elements for stereogram application," J. Disp. Technol. **9**, 607–612 (2013).
10. J. W. Goodman, *Speckle Phenomena in Optics: Theory and Applications* (Roberts, 2009).
11. Y. S. Kim, T. Kim, S. S. Woo, H. Kang, T. C. Poon, and C. Zhou, "Speckle-free digital holographic recording of a diffusely reflecting object," Opt. Express **21**, 8183–8189 (2013).

12. A. Uzan, Y. Rivenson, and A. Stern, "Speckle denoising in digital holography by nonlocal means filtering," Appl. Opt. **52**, A195–A200 (2013).
13. J. M. Artigas, A. Felipe, and M. J. Buades, "Contrast sensitivity of the visual system in speckle imagery," J. Opt. Soc. Am. A **11**, 2345–2349 (1994).
14. Y. Y. Chen, J. H. Wang, C. C. Lin, and H. E. Hwang, "Lensless optical data hiding system based on phase encoding algorithm in the Fresnel domain," Appl. Opt. **52**, 5247–5255 (2013).
15. H. T. Chang, H. E. Hwang, C. L. Lee, and M. T. Lee, "Wavelength multiplexing multiple-image encryption using cascaded phase-only masks in the Fresnel transform domain," Appl. Opt. **50**, 710–716 (2011).
16. A. Ashok and M. A. Neifeld, "Pseudorandom phase masks for superresolution imaging from subpixel shifting," Appl. Opt. **46**, 2256–2268 (2007).
17. Q. L. Deng, Y. S. Chang, G. S. Huang, W. C. Su, and C. Y. Chen, "Despeckle of combined MGSA and a diffuser in digital holographic projection," in *Digital Holography and Three-Dimensional Imaging*, OSA Technical Digest (online) (Optical Society of America, 2013), paper DTh1A.5.
18. C. Y. Chen, W. C. Su, C. H. Lin, M. D. Ke, Q. L. Deng, and K. Y. Chiu, "Reduction of speckles and distortion in projection system by using a rotating diffuser," Opt. Rev. **19**, 440–443 (2012).
19. B. Redding, G. Allen, E. R. Dufresne, and H. Cao, "Low-loss high-speed speckle reduction using a colloidal dispersion," Appl. Opt. **52**, 1168–1172 (2013).
20. H. E. Hwang, H. T. Chang, and W. N. Lie, "Multiple-image encryption and multiplexing using a modified Gerchberg–Saxton algorithm and phase modulation in Fresnel-transform domain," Opt. Lett. **34**, 3917–3919 (2009).
21. H. E. Hwang, H. T. Chang, and W. N. Lai, "Fast double-phase retrieval in Fresnel domain using modified Gerchberg–Saxton algorithm for lensless optical security systems," Opt. Express **17**, 13700–13710, (2009).
22. R. W. Gerchberg and W. O. Saxton, "A practical algorithm for the determination of phase from image and diffraction plane pictures," Optik **35**, 237–246 (1972).
23. B. Julesz, "Cyclopean perception and neurophysiology," Invest. Ophthalmol. Vis. Sci. **11**, 540–548 (1972).
24. J. P. Liu, W. Y. Hsieh, T. C. Poon, and P. Tsang, "Complex Fresnel hologram display using a single SLM," Appl. Opt. **50**, H128–H135 (2011).
25. C. García, I. Pascual, and A. Fimia, "Diffraction efficiency and signal-to-noise ratio of diffuse-object holograms in real time in polyvinyl alcohol photopolymers," Appl. Opt. **38**, 5548–5551 (1999).
26. K. Choi, H. Kim, and B. Lee, "Synthetic phase holograms for auto-stereoscopic image display using a modified IFTA," Opt. Express **12**, 2454–2462 (2004).
27. J. C. Dainty, *Laser Speckle and Related Phenomena* (Springer-Verlag, 1984).
28. L. Wang, T. Tschudi, T. Halldorsson, and P. R. Petursson, "Speckle reduction in laser projection systems by diffractive optical elements," Appl. Opt. **37**, 1770–1775 (1998).
29. F. Riechert, G. Bastian, and U. Lemmer, "Laser speckle reduction via colloidal-dispersion dispersion filled projection screens," Appl. Opt. **48**, 3742–3749 (2009).